Hindawi Publishing Corporation
Journal of Nanomaterials
Volume 2016, Article ID 5849018, 6 pages
http://dx.doi.org/10.1155/2016/5849018

Research Article

Synthesis and Characterization of Polymeric Graphene Quantum Dots Based Nanocomposites for Humidity Sensing

Lam Minh Long,[1,2] Nguyen Nang Dinh,[1] and Tran Quang Trung[3]

[1]*University of Engineering and Technology, Vietnam National University Hanoi, 144 Xuan Thuy, Hanoi 10000, Vietnam*
[2]*Ho Chi Minh City Vocational College, 38 Tran Khanh Du, District 1, Ho Chi Minh City 10001, Vietnam*
[3]*University of Natural Science, Vietnam National University, Ho Chi Minh City, 227 Nguyen Van Cu Road, District 5, Ho Chi Minh City 10001, Vietnam*

Correspondence should be addressed to Nguyen Nang Dinh; dinh158@yahoo.com

Received 22 January 2016; Accepted 27 March 2016

Academic Editor: Mingqiang Li

Graphene quantum dots (GQDs) were synthesized and incorporated with polyethylenedioxythiophene:poly(4-styrenesulfonate) (PEDOT:PSS) and carbon nanotube (CNT) to form a composite that can be used for humidity sensors. The 600 nm thick composite films contained bulk heterojunctions of CNT/GQD and CNT/PEDOT:PSS. The sensors made from the composites responded well to humidity in a range from 60 to 80% at room temperature and atmospheric pressure. With a CNT content of 0.4 wt.% (GPC-1) to 0.8 wt.% (GPC-2) and 1.2 wt.% (GPC-3), the sensitivity of the humidity sensing devices based on CNT-doped graphene quantum dot-PEDOT:PSS composites was increased from 4.5% (GPC-1) to 9.0% (GPC-1) and 11.0% (GPC-2), respectively. The fast response time of the GPC sensors was about 20 s and it was much improved due to CNTs doping in the composites. The best value of the recovery time was found to be of 40 s, for the GPC composite film doped with 1.2 wt.% CNT content.

1. Introduction

Nanocomposites are known as materials mixing two or more different materials, where at least one of these has a nanodimensional phase, for example, conjugate polymers embedded with metallic, semiconducting, and dielectric nanoparticles. In comparison with devices made from standard materials, the nanocomposites-based devices usually possess enhanced efficiency and service life [1–4]. This is because inorganic nanoparticles embedded in conducting polymers can improve the mechanical, electrical, and optical properties such as nonlinear optical behavior, photoluminescence, electroluminescence, and photoconductivity [5–7]. Nanostructured composites or nanohybrid layers containing numerous heterojunctions can be utilized for optoelectronics, organic light emitting diodes (OLEDs), organic solar flexible cells (OSC) [8, 9], and so forth. Among conducting polymers, polyethylenedioxythiophene:poly(4-styrenesulfonate) (abbreviated to PEDOT:PSS) as a p-type organic semiconductor is well used for the hole transport layer in OLED [10] and OSC [4] as well as for the matrices materials in various sensors [11]. Various nanocomposite films consisting of conducting polymers mixed with carbon nanotubes (CNTs) as an active material have been prepared for application in gas thin film sensors. Recently, Olenych et al. [12] used hybrid composites based on PEDOT:PSS-porous silicon-CNT for preparation and characterization of humidity sensors. The value of the resistance of the hybrid films was as large as 10 MΩ that may have caused a reduced accuracy in monitoring the resistance change versus humidity.

It is known that graphene possesses many excellent electrical properties, since it is an allotrope of carbon with a structure of a single two-dimensional (2D) layer of sp^2 hybridized carbon atoms. Graphene quantum dots (GQDs), as seen in [13, 14], are a kind of 0D material made from small pieces of graphene. GQDs exhibit new phenomena due to quantum confinement and edge effects, which are similar to semiconducting QDs [15]. Graphene and related materials like graphene oxide (GO) or reduced graphene oxide (rGO) as materials used for chemical sensing have significant application potential. This is due to the 2-dimensional structure

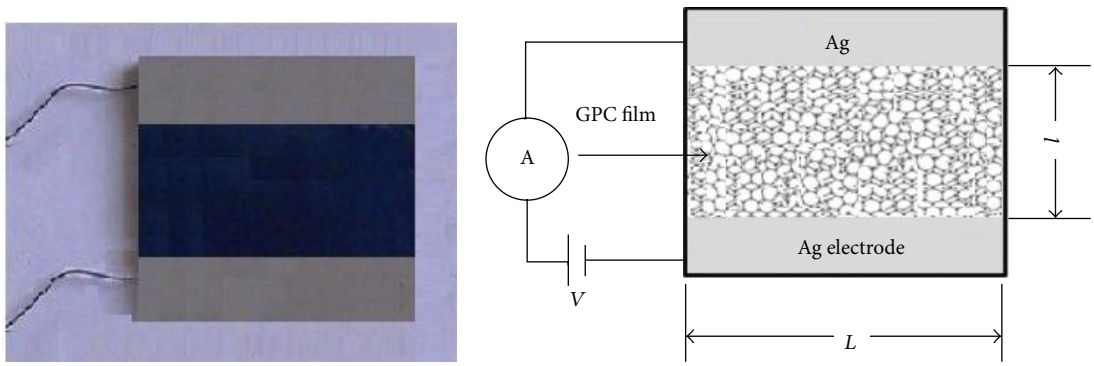

Figure 1: Image of a humidity sensor made from a single layer of PEDOT:PSS+GQDs+CNT composite film (a) and the schematic drawing of the device with the two planar electrodes (b). Humidity change is detected by the change in the current with a constant Dc-bias applied to the two electrodes.

that results in a high sensing area per unit volume and a low noise compared to other solid state sensors. There were many works reporting on the use of graphene or graphene related materials for monitoring gases and vapors [16, 17]. Particularly, some of the works attempted to connect the advantages of nanoscale metals with that of graphene for the improvement of gas sensor applications [18, 19]. GQDs were mainly used in a single electron transistor (SET). Besides detecting charge in SETs, GQDs have also been recruited to build electronic sensors for the detection of humidity and pressure [20].

In this work we report results of our investigation on the fabrication of graphene quantum dots and nanocomposites of PEDOT:PSS+GQDs+CNT. The humidity sensing properties of the PEDOT:PSS+GQDs+CNT composite based thin film sensors are also presented.

2. Experimental

2.1. Preparation of GQDs and CNT-Doped GQDs+PEDOT:PSS Composites. To prepare GQDs, a solution of graphite flake (GF), $KMnO_4$, and HNO_3 with a weight ratio of 0.2 g : 0.2 g : 0.4 mL was prepared and put in a Pt crucible. This solution was then put in a microwave oven for heating for 1 min to separate GF into laminar form (EG). The second solution was made from 0.2 g $NaNO_3$ + 9.6 mL H_2SO_4 (98%) + 1,2 g $KMnO_4$ (called as NKH). EG was mixed with NKH solution and carefully stirred by use of a magnetic device for 2 h to have a GO solution. Adding to the GO solution 30 mL distilled water and then 10 mL H_2O_2 allowed us to get a dark-yellow solution. By spinning with a rate of 7000 rpm for 5 min, a GO powder was obtained and it was diluted in deionized water. In the next step, NH_3 was added in the solution and stirred at 100°C for 5 h until a solution with a uniform dispersion of GQDs was reached. Finally, the GQDs dispersed solution was filtrated by using the "Dialysis" funnel to collect a GQDs powder with a volume of 0.2 g. This powder then was dissolved in 20 mL of twice-distilled water to get a GQDs-dispersion solution of 10 wt.% GQDs (abbreviated to GQD10).

To prepare the GQDs+PEDOT:PSS composite solution, firstly a powder of multiple wall carbonate tubes (shortly abbreviated to CNT) with an average size of 30 nm in diameter and 2 μm in length was embedded in 10 mL of the GQD10 solution without CNT and with three contents of CNT, respectively, 0.5 mg, 1.0 mg, and 1.5 mg. All of the solutions obtained are called GQC solutions. These solutions were treated by plasma in a microwave oven. Then 2 mL of PEDOT:PSS (1.25 wt.% in H_2O) was poured into each GQC solution. The solutions of GQDs-PEDOT:PSS without and with CNT of the three abovementioned volumes of CNT were stirred by ultrasonic wave for 1 hour. Using spin-coating, four GQC solutions were deposited onto glass substrates which were coated by two silver planar electrode arrays with a length (L) of 10 mm and separated from one another by a distance (l) of 5 mm, as shown in Figure 1. In the spin-coating technique used for preparing composite films, the following parameters were chosen: a delay time of 100 s, a rest time of 45 s, a spin speed of 1500–1800 rpm, an acceleration of 500 rpm, and finally a drying time of 3 min. To dry the composite films, a flow of dried gaseous nitrogen was used for 10 hours. For a solidification avoiding the use of solvents, the film samples were annealed at 120°C for 8 h in a "SPT-200" vacuum drier. From all the volumes of chemicals such as GQDs, PEDOT:PSS, and CNT used for the films preparation, the CNT weight contents (wt.%) in the GQDs-PEDOT:PSS matrix have been calculated. It is seen that the samples embedded with the CNT volume of 0.5 mg, 1.0 mg, and 1.5 mg consist of 0.4 wt.%, 0.8 wt.%, and 1.2 wt.%, respectively. For simplicity in further analysis, the samples without and with CNT of 0.4 wt.%, 0.8 wt.%, and 1.2 wt.% were abbreviated to GPC-0, GPC-1, GPC-2, and GPC-3, respectively. Finally, these film samples were kept in a dry Ar glove-box until the measurements.

2.2. Characterization Techniques. The thickness of the films was measured on a "Veeco Dektak 6M" stylus profilometer. The size of GQDs and the surface morphology of the films were characterized by using "Hitachi" Transmission Electron Microscopy (TEM) and Emission Scanning Electron

Microscopy (FE-SEM), respectively. For humidity sensing measurements, the samples were put in a 10 dm^3-volume chamber; a humidity value could be fixed in a range from 20% to 80% by the use of a "EPA-2TH" moisture profilometer (USA). The adsorption process is controlled by insertion of water vapor, while the desorption process was done by extraction of the vapor followed by insertion of dry gaseous Ar. The measurement system that was described in [21] consists of an Ar gas tank, gas/vapor hoses and solenoids system, two flow meters, a bubbler with vapor solution, and an airtight test chamber connected with collect-store data DAQ component. The Ar gas played a role as carrier gas, dilution gas, and purge gas.

For each sample, the number of measuring cycles was chosen to be at least 10 cycles. The humidity flow taken for measurements was of ~60 sccm mL/min. The sheet resistance of the samples was measured on a "KEITHLEY 2602" system source meter.

3. Results and Discussion

3.1. Electrical Properties and Morphology. From a TEM micrograph of a GQDs sample (Figure 2), it is seen that the size distribution of the dots is considerably homogenous; as evaluated in this micrograph, the dots size ranged from 10 nm to 15 nm. Figure 3 is a FE-SEM micrograph of the GPC-3 sample where the CNT and GQDs clearly appeared while the conjugate polymer PEDOT:PSS exhibited a transparent matrix. This SEM micrograph also shows that in the GPC composite film there are mainly heterojunctions of the GQD/PEDOT-PSS and CNT/PEDOT:PSS, whereas CNT/GQD junctions are rarely formed.

From the thickness measurements, it can be seen that embedding CNT made the GPC samples considerably thicker. However, for the CNT-embedded GPC films, the CNT concentration was not much affected by the film thickness, so that the change in the thickness versus CNT concentration could be neglected. Indeed, for GPC-0 samples (i.e., the samples without CNT) the value of the film thickness was found to be ~5% smaller than that of the GPC + CNT samples (Table 1). This can be explained by the lower viscosity of GPC solution in comparison with the viscosity of GPC composite solutions. The results of measurements of the sheet resistance (R) of the samples are listed in Table 1.

For thin films, the sheet resistance in the investigated samples can be expressed as follows:

$$R_s = \rho \frac{l}{S} = \rho \frac{l}{2l \times d} = \frac{\rho}{2d}, \quad (1)$$

where l is the separation distance between two Ag electrodes, $S = L \times d = 2l \times d$.

Thus from the sheet resistance one can determine the resistivity (ρ) of the films as follows:

$$\rho = 2R_s \times d. \quad (2)$$

Thus, the conductivity (σ) is

$$\sigma \sim \frac{1}{\rho} = \frac{1}{2R_s d}. \quad (3)$$

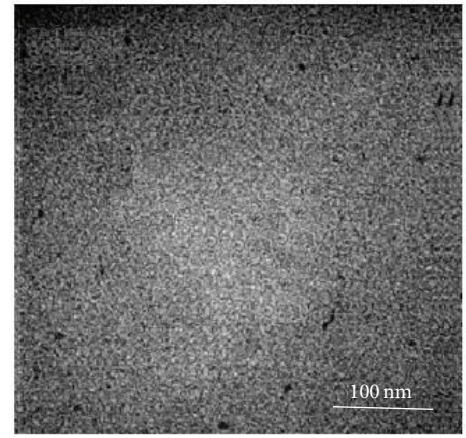

Figure 2: TEM micrograph of a GQDs sample.

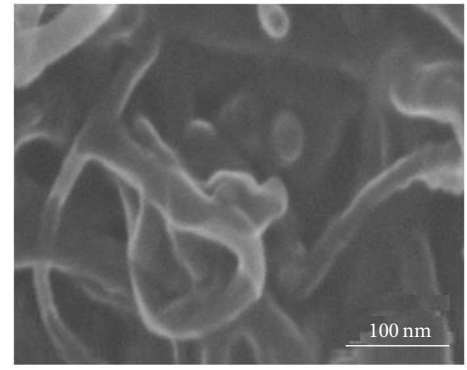

Figure 3: FE-SEM micrograph of the GPC-3 composite sample.

Table 1: Thickness and resistance at room temperature of graphene quantum dots/CNT composite films.

Samples	CNT content (wt%)	Thickness, d (nm)	R_s (kΩ)	Conductivity, σ (S/cm)
GPC-0	0	460	2.180	4.98
GPC-1	0.4	485	2.160	4.76
GPC-2	0.8	487	0.814	7.93
GPC-3	1.2	490	0.356	27.52

The values of the conductivity of the composited films calculated by formula (3) are shown in Table 1. The conductivity of the GPC-3 film is the largest and can be compatible to the conductivity of a pure PEDOT-PSS film as reported in [22]. Embedding GQDs and CNT into PEDOT-PSS has made the conductivity of PEDOT-PSS decrease, leading to the expectation that the sensitivity of the GPC composite films would be enhanced.

The temperature dependence of the conductivity of GPC samples is shown in Figure 4. For GPC-1 sample, σ versus T curves exhibit a typical property of the inorganic semiconductors: with increases in temperature the conductivity increases. With increases in the CNT content, the composite

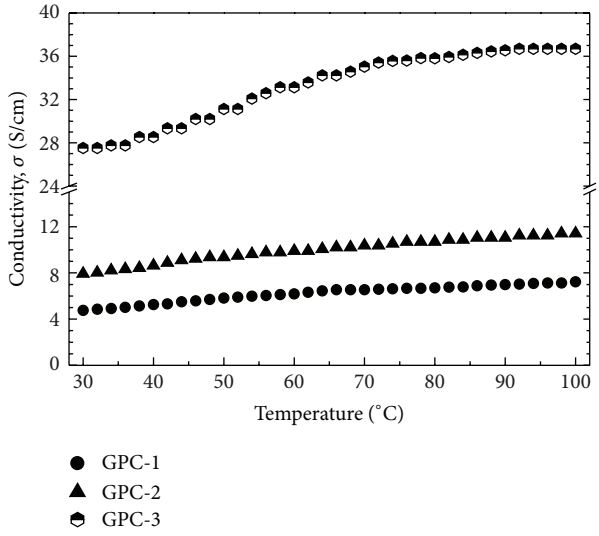

Figure 4: Temperature dependence of the conductivity of GPC-1, GPC-2, and GPC-3 films.

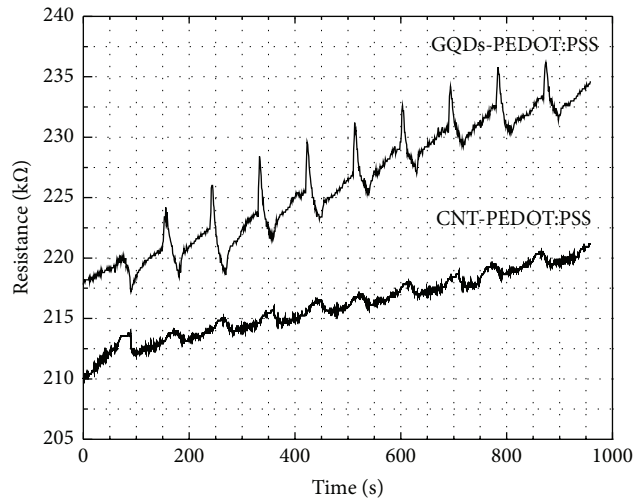

Figure 5: Sheet resistance change versus humidity of GQDs-PEDOT:PSS and CNT-PEDOT:PSS composite films during adsorption/desorption processes.

exhibited a clearer semiconductor behavior; and when it reached a value as large as 1.2 wt.% (namely, in GPC-3 sample), the conductivity of the films maintained an almost unchanged value of 37.2 S/cm under elevated operating temperatures. This thermal stability property is a desired factor for materials that are used in sensing applications.

3.2. Humidity Sensing Characterization. To characterize humidity sensitivity of the GPC samples, the devices were placed in a test chamber and device electrodes were connected to electrical feedthroughs. The measurements included two processes: adsorption and desorption. In the adsorption process, the humidity flow consisting of Ar carrier and H_2O vapor from a bubbler was introduced into the test chamber for an interval of time, following which the change in resistance of the sensors was recorded. In the desorption process, a dried Ar gas flow was inserted in the chamber in order to recover the initial resistance of the GPC films. Through the recovering time dependence of the resistance one can obtain information on the desorption ability of the sensor in the desorption process.

Figure 5 demonstrates the adsorption and desorption processes of the GQDs-PEDOT:PSS and CNT-PEDOT:PSS sensors. This figure shows that in the first 60 s Ar gaseous flow eliminated the contamination agents from the GQDs-PEDOT:PSS surface; consequently the surface resistance increased. After the cleaning of the sensor surface during 30 s, the introduced humidity vapor was adsorbed onto the sensor surface, resulting in the decrease of the resistance. In the subsequent cycles, the humidity desorption/adsorption process led, respectively, to increase and decrease of the resistance of sensors, with results similar to those reported in [11]. However, through each cycle, the resistance of the GQDs-PEDOT:PSS film did not recover/restore to its initial value but increased in 1 to 2 kΩ, to a final value of 235 kΩ after 1000 s from 220 kΩ. The increase in the initial resistance of the GQDs-PEDOT:PSS mainly related to the decrease of the major charge carriers in PEDOT:PSS. This is due to the elimination of holes (as the major carriers in PEDOT:PSS) by electrons that were generated from the H_2O adsorption. The more desorption/adsorption cycles, the more holes eliminated in the deeper distances in the composite films. The similar feature in the sheet resistance change versus humidity was observed for the CNT-PEDOT:PSS, but the sensitivity of the last was much less than the one of the GQDs-PEDOT:PSS sensor. This proves the advantage of GQDs embedded in PEDOT:PSS polymer for the humidity sensing.

To appreciate better the sensing performance of the GPC composite films used for the sensors, a sensitivity (η) of the devices was introduced. It is determined by the following equation:

$$\eta = \frac{R - R_0}{R_0} \ (\%) . \tag{4}$$

The absolute magnitude of the sensitivity of the GPC-0 calculated by formula (4) is of ca. 2.5%.

Plots of time dependence of the sensitivity of the CNT-doped GPC composite films are shown in Figure 6. From this figure one can see that, for the GPC samples, opposite to the GQDs-PEDOT:PSS, the humidity (i.e., H_2O vapor) adsorption process led to increase in the resistance of the films. Moreover the resistance increased at a much faster rate than when it decreased.

Looking at the humidity sensing curves in Figure 6, one can distinguish two phenomena: the "rapid" (steep slope) and "slow" (shallow slope) response. The rapid response arises from H_2O molecular adsorption onto low-energy binding sites, such as sp^2-bonded carbon, and the slow response arises from molecular interactions with higher energy binding sites, such as vacancies, structural defects, and other functional groups [23, 24].

For the next step, the sensitivity ability of GPC composite was studied and the whole experiment process as described

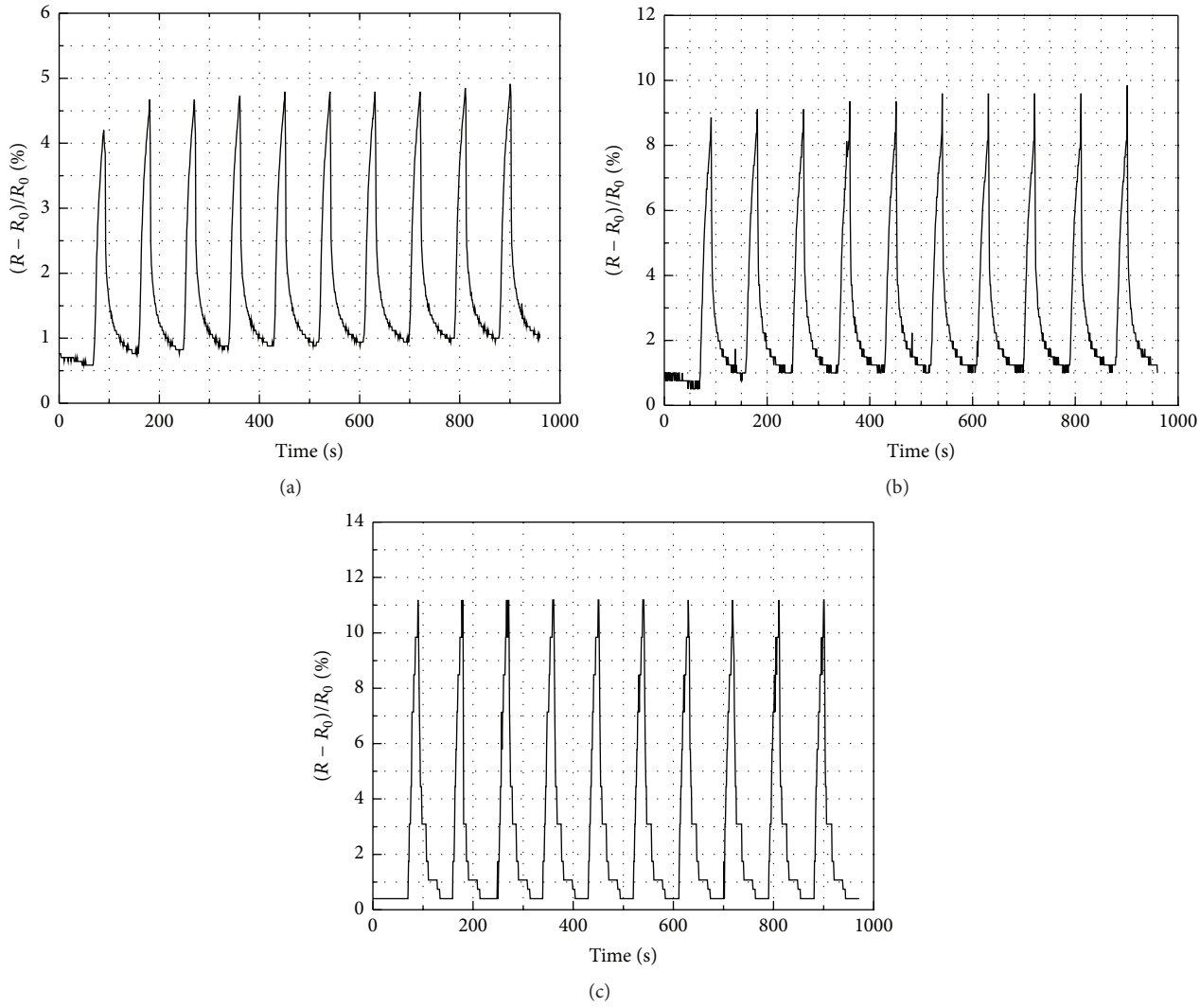

Figure 6: Comparison of the humidity sensing of the GPC composite based sensors versus CNT content; (a) GPC-1 (0.4 wt.%), (b) GPC-2 (0.8 wt.%), and (c) GPC-3 (1.2 wt.%).

above was repeated. The data in Figure 6 show that the presence of CNT can improve the sensing properties of GPC sheets. With increase in the CNT content, the resistivity increased, from 4.5% (for GPC-1) to 9.0% (for GPC-2) and 11.0% (for GPC-3).

The response time (i.e., the duration for R_0 raising up to R_{max} in the adsorption process) for all three GPC sheets is almost the same value of 20 s, whereas the recovery time (the duration for R_0 lowering to R_{max} in the desorption process) decreased from 70 s (GPC-1, Figure 6(a)) to 60 s (GPC-2, Figure 6(b)) and 40 s (GPC-3, Figure 6(c)). In addition, the complete H_2O molecular desorption on the surface of GPC composites took place at room temperature and atmospheric pressure. One can guess that connecting together individual GPC sheets by CNTs caused the increase of the mobility of carriers in GPC composite films, consequently leading to higher H_2O vapor sensing ability of the CNT-doped GQDs-PEDOT:PSS composites. Indeed, due to the appearance of CNTs bridges, the number of the sites with high binding energies in GPC sheets decreases, while the number of those with low binding energies increases. Since the H_2O molecules was mainly adsorbed at the sites with low binding energies, the appearance of CNTs bridges led to the complete desorption ability of GPC composites.

4. Conclusion

The synthesized graphene quantum dots (GQDs) and spin-coated composite thin films of GQDs, PEDOT:PSS, and CNT (GPC) were used for preparing humidity sensors. The sensors had extremely simple structure and they responded well to the humidity change at room temperature and atmospheric pressure. With the CNT content increase, from 0% (GPC-0) to 0.4 wt.% (GPC-1), 0.8 wt.% (GPC-2), and 1.2 wt.% (GPC-3), the sensitivity of the humidity sensing devices based on CNT-doped graphene quantum dot-PEDOT:PSS composites improved from 2.5% (GPC-0) to 4.5% (GPC-1), 9.0% (GPC-1), and 11.0% (GPC-2), respectively. The response time the

GPC sensors was as fast as 20 s; and the recovery time of the sensors lowered from 70 s (0.4 wt.% CNT) to 60 s (0.8 wt.% CNT) and 40 s (1.2 wt.% CNT).

Competing Interests

The authors declare that there are no competing interests related to this paper.

Acknowledgments

This research was funded by the Vietnam National Foundation for Science and Technology (NAFOSTED) under Grant no. 103.02-2013.39. The authors express sincere thanks to Professor Vo-Van Truong (Department of Physics, Concordia University, Canada) for useful discussion.

References

[1] T. P. Selvin, J. Kuruvilla, and T. Sabu, "Mechanical properties of titanium dioxide-filled polystyrene microcomposites," *Materials Letters*, vol. 58, no. 3-4, pp. 281–289, 2004.

[2] J. Móczó and B. Pukánszky, "Polymer micro and nanocomposites: structure, interactions, properties," *Journal of Industrial & Engineering Chemistry*, vol. 14, no. 5, pp. 535–563, 2008.

[3] S. A. Choulis, M. K. Mathai, and V.-E. Choong, "Influence of metallic nanoparticles on the performance of organic electrophosphorescence devices," *Applied Physics Letters*, vol. 88, Article ID 213503, 2006.

[4] T. T. Thao, T. Q. Trung, V.-V. Truong, and N. N. Dinh, "Enhancement of power efficiency and stability of P3HT-based organic solar cells under elevated operatingeratures by using a nanocomposite photoactive layer," *Journal of Nanomaterials*, vol. 2015, Article ID 463565, 7 pages, 2015.

[5] W. U. Huynh, J. J. Dittmer, and A. P. Alivisatos, "Hybrid nanorod-polymer solar cells," *Science*, vol. 295, no. 5564, pp. 2425–2427, 2002.

[6] A. Petrella, M. Tamborra, P. D. Cozzoli et al., "TiO_2 nanocrystals—MEH-PPV composite thin films as photoactive material," *Thin Solid Films*, vol. 451-452, pp. 64–68, 2004.

[7] V. M. Burlakov, K. Kawata, H. E. Assender, G. A. D. Briggs, A. Ruseckas, and I. D. W. Samuel, "Discrete hopping model of exciton transport in disordered media," *Physical Review B*, vol. 72, Article ID 075206, 2005.

[8] J. Ouyang, Q. Xu, C.-W. Chu, Y. Yang, G. Li, and J. Shinar, "On the mechanism of conductivity enhancement in poly(3,4-ethylenedioxythiophene):poly(styrene sulfonate) film through solvent treatment," *Polymer*, vol. 45, no. 25, pp. 8443–8450, 2004.

[9] P. Tehrani, A. Kanciurzewska, X. Crispin, N. D. Robinson, M. Fahlman, and M. Berggren, "The effect of pH on the electrochemical over-oxidation in PEDOT:PSS films," *Solid State Ionics*, vol. 177, no. 39-40, pp. 3521–3527, 2007.

[10] M. Sain, S. Ummartyotin, J. Juntaro, C. Wu, and H. Manuspiya, "Deposition of PEDOT: PSS nanoparticles as a conductive microlayer anode in OLEDs device by desktop inkjet printer," *Journal of Nanomaterials*, vol. 2011, Article ID 606714, 7 pages, 2011.

[11] J. N. Gavgani, H. S. Dehsari, A. Hasani et al., "A room temperature volatile organic compound sensor with enhanced performance, fast response and recovery based on N-doped graphene quantum dots and poly(3,4-ethylenedioxythiophene)–poly(styrenesulfonate) nanocomposite," *RSC Advances*, vol. 5, no. 71, pp. 57559–57567, 2015.

[12] I. B. Olenych, O. I. Aksimentyeva, L. S. Monastyrskii, Y. Y. Horbenko, and L. I. Yarytska, "Sensory properties of hybrid composites based on poly(3,4-ethylenedioxythiophene)-porous silicon-carbon nanotubes," *Nanoscale Research Letters*, vol. 10, article 187, 2015.

[13] J. Shen, Y. Zhu, X. Yang, and C. Li, "Graphene quantum dots: emergent nanolights for bioimaging, sensors, catalysis and photovoltaic devices," *Chemical Communications*, vol. 48, no. 31, pp. 3686–3699, 2012.

[14] Z. P. Zhang, J. Zhang, N. Chen, and L. T. Qu, "Graphene quantum dots: an emerging material for energy-related applications and beyond," *Energy and Environmental Science*, vol. 5, no. 10, pp. 8869–8890, 2012.

[15] L. Li, G. Wu, G. Yang, J. Peng, J. Zhao, and J.-J. Zhu, "Focusing on luminescent graphene quantum dots: current status and future perspectives," *Nanoscale*, vol. 5, no. 10, pp. 4015–4039, 2013.

[16] S. Basu and P. Bhattacharyya, "Recent developments on graphene and graphene oxide based solid state gas sensors," *Sensors and Actuators B: Chemical*, vol. 173, pp. 1–21, 2012.

[17] P. T. Yin, T.-H. Kim, J.-W. Choi, and K.-B. Lee, "Prospects for graphene-nanoparticle-based hybrid sensors," *Physical Chemistry Chemical Physics*, vol. 15, no. 31, pp. 12785–12799, 2013.

[18] B. H. Chu, J. Nicolosi, C. F. Lo, W. Strupinski, S. J. Pearton, and F. Ren, "Effect of coated platinum thickness on hydrogen detection sensitivity of graphene-based sensors," *Electrochemical and Solid-State Letters*, vol. 14, no. 7, pp. K43–K45, 2011.

[19] M. Zhang and Z. Wang, "Nanostructured silver nanowires-graphene hybrids for enhanced electrochemical detection of hydrogen peroxide," *Applied Physics Letters*, vol. 102, no. 21, pp. 213104–213106, 2013.

[20] T. S. Sreeprasad, A. A. Rodriguez, J. Colston et al., "Electron-tunneling modulation in percolating network of graphene quantum dots: fabrication, phenomenological understanding, and humidity/pressure sensing applications," *Nano Letters*, vol. 13, no. 4, pp. 1757–1763, 2013.

[21] Q. T. Tran, M. H. H. Tran, D. T. Tong, V. T. Tran, and N. D. Nguyen, "Synthesis and application of graphene-silver nanowires composite for ammonia gas sensing," *Advances in Natural Sciences: Nanoscience and Nanotechnology*, vol. 4, no. 4, 2013.

[22] J. Ouyang, C.-W. Chu, F.-C. Chen, Q. Xu, and Y. Yang, "High-conductivity poly(3,4-ethylenedioxythiophene):poly(styrene sulfonate) film and its application in polymer optoelectronic devices," *Advanced Functional Materials*, vol. 15, no. 2, pp. 203–208, 2005.

[23] G. Lu, S. Park, K. Yu et al., "Toward practical gas sensing with highly reduced graphene oxide: a new signal processing method to circumvent run-to-run and device-to-device variations," *ACS Nano*, vol. 5, no. 2, pp. 1154–1164, 2011.

[24] J. T. Robinson, F. K. Perkins, E. S. Snow, Z. Wei, and P. E. Sheehan, "Reduced graphene oxide molecular sensors," *Nano Letters*, vol. 8, no. 10, pp. 3137–3140, 2008.